Yesiller, et al., Published in Waste Management, 42: 166-179. August 2015.

Waste heat generation: A comprehensive review

Nazli Yeşiller [a,*], James L. Hanson [b,1], Emma H. Yee [c,2]

[a] Global Waste Research Institute, California Polytechnic State University, San Luis Obispo, CA 93407, USA
[b] Civil and Environmental Engineering Department, California Polytechnic State University, San Luis Obispo, CA 93407, USA
[c] Chemical Engineering Department, Columbia University, New York, NY 10027, USA

ARTICLE INFO

Keywords:
Municipal solid waste
Mining waste
Incinerator ash
Temperature
Thermal property
Heat generation

ABSTRACT

A comprehensive review of heat generation in various types of wastes and of the thermal regime of waste containment facilities is provided in this paper. Municipal solid waste (MSW), MSW incineration ash, and mining wastes were included in the analysis. Spatial and temporal variations of waste temperatures, thermal gradients, thermal properties of wastes, average temperature differentials, and heat generation values are provided. Heat generation was influenced by climatic conditions, mean annual earth temperatures, waste temperatures at the time of placement, cover conditions, and inherent heat generation potential of the specific wastes. Time to onset of heat generation varied between months and years, whereas timelines for overall duration of heat generation varied between years and decades. For MSW, measured waste temperatures were as high as 60–90 °C and as low as −6 °C. MSW incinerator ash temperatures varied between 5 and 87 °C. Mining waste temperatures were in the range of −25 to 65 °C. In the wastes analyzed, upward heat flow toward the surface was more prominent than downward heat flow toward the subsurface. Thermal gradients generally were higher for MSW and incinerator ash and lower for mining waste. Based on thermal properties, MSW had insulative qualities (low thermal conductivity), while mining wastes typically were relatively conductive (high thermal conductivity) with ash having intermediate qualities. Heat generation values ranged from −8.6 to 83.1 MJ/m^3 and from 0.6 to 72.6 MJ/m^3 for MSW and mining waste, respectively and was 72.6 MJ/m^3 for ash waste. Conductive thermal losses were determined to range from 13 to 1111 MJ/m^3 yr. The data and analysis provided in this review paper can be used in the investigation of heat generation and thermal regime of a wide range of wastes and waste containment facilities located in different climatic regions.

1. Introduction

Heat, in addition to gas and leachate, is a primary byproduct of disposal of different types of solid wastes. Examples of heat generation and elevated temperatures in MSW were reported by Yeşiller et al. (2005) and Hanson et al. (2010). Heat generation in waste incinerator ash was documented in Klein et al. (2001). For mining wastes, data were reported, for example, by Lefebvre et al. (1997) and Hollesen et al. (2011). Heat is generated as a result of biochemical processes and decomposition of organic constituents in wastes as well as due to chemical reactions that occur within the wastes. Heat generation and waste temperatures are coupled to concurrent biochemical processes and chemical reactions as well as affect mechanical and hydraulic properties and behavior of the wastes. In addition, waste temperatures influence engineering properties and behavior of bottom liners, covers, and surrounding subgrade soils.

Temperatures affect decomposition of MSW through two pathways: short-term effects on reaction rates and long-term effects on microbial population balance (Hartz et al., 1982). In general, waste decomposition increases with increasing temperatures up to limiting values. In laboratory studies, optimum temperature ranges for the growth of mesophilic and thermophilic bacteria responsible for waste decomposition were identified to be 35–40 °C and 50–60 °C, respectively (Tchobanoglous et al., 1993; Cecchi et al., 1993). Maximum gas production from waste decomposition was identified to occur at temperature ranges between 34 and 41 °C based on laboratory analysis (Merz, 1964 and Ramaswamy, 1970 as reported in DeWalle et al., 1978; Hartz et al., 1982; Mata-Alvarez and Martinez-Viturtia, 1986). A temperature range of 40–45 °C was identified as the optimum range for gas production at a landfill in England (Rees, 1980a,b) with highly inhibited and delayed gas

* Corresponding author. Tel.: +1 805 756 2932; fax: +1 805 756 6330.
E-mail addresses: nyesille@calpoly.edu (N. Yeşiller), jahanson@calpoly.edu (J.L. Hanson), emma.o.yee@gmail.com (E.H. Yee).
[1] Tel.: +1 805 756 6227; fax: +1 805 756 6330.
[2] Tel.: +1 512 923 8200.

generation observed at low waste temperatures (Hanson et al., 2006). Biomass transfer was reported to occur with landfill gas, where the cell counts in the gas were correlated to temperature (Barry, 2008). Spatially unique microbial communities, as influenced by waste temperature among other factors, were reported in landfill environments (Sawamura et al., 2010). Temperature and heat generation effects on waste decomposition and emissions from containment facilities were included in modeling of landfill processes and mass transport in various studies (e.g., El-Fadel et al., 1996; Kjeldsen and Christensen, 2001; Lowry et al., 2008; Spokas et al., 2011).

Temperatures also affect engineering properties of wastes and properties and performance of earthen and geosynthetic components of cover and bottom liner systems. Compressibility of MSW increased nearly twofold for a temperature change from 20 to 35 °C in laboratory tests (Lamothe and Edgers, 1994). Similarly, magnitude and rate of settlement increased with temperature in a modeling study of long-term settlement of MSW (Chakma and Mathur, 2013). Increased compressibility indicates a potential decrease in shear strength of wastes, which may affect stability of waste slopes. Hudson (2007) indicated that temperature might affect hydraulic conductivity of wastes in addition to stress and permeant fluid properties and that differences (increasing hydraulic conductivity with increasing temperature) in excess of 50% could be expected for waste temperature variations on the order of 20 °C. Elevated temperatures can increase diffusive and advective transport through liner systems, accelerate various degradation processes (i.e., oxidation, hydrolysis, chemical, etc.) and aging of geosynthetics, cause desiccation of earthen materials, influence pore structure and fluid transport characteristics, and increase clogging rates of leachate collection systems (e.g., Southen and Rowe, 2005; Ishimori and Katsumi, 2012; Abuel-Naga and Bouazza, 2013; Koerner and Koerner, 2014).

Thermal conditions for mining wastes typically have been investigated in relation to acid mine drainage from waste rock materials and tailings generated from various mining operations (e.g., Lefebvre et al., 2001; Sracek et al., 2004; Hollesen et al., 2009; Pham et al., 2013). Sulfides common in mining wastes are oxidized in bacterially mediated highly exothermic reactions leading to heat generation in mine waste piles. Pyrite (FeS_2) is a naturally occurring sulfide mineral present in the earth's crust and is commonly encountered in waste rocks or tailings generated during extraction or treatment of various types of ores. Pyrite is oxidized by direct reaction with oxygen and water or is oxidized by ferric iron (Lefebvre et al., 1997). Coupled biogeochemical processes affect overall heat transfer and temperature trends in mine wastes (e.g., Lefebvre et al., 2001). Significant pyrite oxidation occurs when the pyrite in the waste rock or tailings is exposed to environmental conditions. The biochemical pyrite oxidation reaction is influenced by availability of oxygen and water, and the heat generated in the process and the varying temperature of the environment in which the reaction takes place in turn affect the rate of oxidation. Optimum temperature ranges for iron-oxidizing bacteria were indicated to be between 25 and 45 °C with a 60–80 °C range representing ideal conditions for thermophilic species (Lefebvre et al., 2001). Increasing temperatures enhance the oxidation reactions leading to increased potential for acid mine drainage and contaminant migration and pollution at elevated temperatures (e.g., Hollesen et al., 2009).

This review was conducted to provide a comprehensive dataset and tools for analysis of temperatures, thermal properties, and heat generation and transfer, in various types of wastes including MSW, MSW incineration ash, and mining wastes. Spatial and temporal temperature trends and associated heat generation values as well as thermal properties for wastes are presented. Data were obtained from investigations conducted by the authors since 1999 for MSW and obtained from studies available in the literature for MSW and other waste types. The data and analysis provided herein can be used in a wide variety of settings to investigate thermally related phenomena in waste containment systems.

2. Waste temperatures

Initially, data are provided for spatial and temporal variations of temperatures in MSW landfills. Next, data are provided for MSW incinerator ash landfills. Finally, data are reported for mining waste piles. Thermal gradients also are included. Data from studies where temperature measurements were made directly in the waste mass were used as much as possible throughout this paper. Temperature measurements obtained using sensors placed in rigid pipes/tubing/holes (i.e., open conduits) filled with air or water/leachate, or measurements obtained on excavated samples or during drilling operations generally were excluded. Further details and discussion regarding effectiveness and representativeness of MSW temperature measurements were provided in Yesiller et al. (2005) and Hanson et al. (2010).

2.1. MSW temperatures

A summary of the location, climatic conditions, and site details for the MSW landfills included in this paper is provided in Table 1. Collection of leachate was indicated for the site in France, no information was provided for the site in Italy, and leachate mounding was indicated for the site in UK. Significant leachate mounding also was reported for the site in Japan. The landfills located in North America had leachate collection and removal systems with varying degrees of sophistication. Temperatures were monitored in a test cell containing only organic waste at the site in Australia, which was indicated to have a leachate collection system. Gas collection systems were installed at the sites located in Italy, France, and North America. While gas concentration and generation rates were provided for the sites in UK and Japan, specific information on the presence of gas collection systems was not provided. Landfill gas was not collected in the organic waste cell used for temperature monitoring at the site in Australia. In general, data were collected in areas covered with daily/intermediate cover at the sites at early stages of data collection soon after waste placement and in areas overlain by intermediate cover when older wastes were monitored. Data were collected from areas with initially daily/interim covers followed by final covers at the landfills located in France and Pennsylvania (USA). Wastes were not covered at the site in Australia.

Variations of waste temperatures with time are presented in Fig. 1a for relatively young wastes (ages < 3.5 years) and in Fig. 1b for older wastes (ages 3–33 years). Temperature data from multiple cells containing wastes with different ages are presented for the Vancouver, Canada landfill site in Fig. 1b. At the MSW sites included in this review, temperatures generally increased over a period of years upon placement and remained relatively stable for extended periods with decreases occurring 5 to over 15 years after initial placement (Fig. 1). In general, higher temperature changes occurred in young wastes than in old wastes. In cases where temperatures increased rapidly, high heat generation likely occurred during aerobic decomposition conditions, whereas for cases with slower temperature increase, continued heat generation occurred during anaerobic conditions.

In temperate climates, maximum waste temperatures on the order of 60–90 °C were measured, whereas typically significantly lower temperatures were measured in cold climates on the order of −6 to 15 °C. High temperatures also were obtained in cold climates (e.g., Michigan, USA) with optimum precipitation of

Table 1
Site description: MSW.

Source	Site/location	Latitude and longitude (°)	Climatic region[a]	Average annual air temperature (°C)	Average annual precipitation (mm)	Waste depth (m)[g]	Waste age (years)
Rees (1980a)	Aveley Landfill (near Essex, UK)	51.74N, 0.47E[b]	Temperate, no dry season, warm summer	*10.5*	*630*	5 to 7	3 to 6
Zanetti et al. (1997)	(Turin, Italy)	45.08N, 7.68E	Temperate, no dry season, hot summer	*11.6*	*917*	24	7 to 13
Houi et al. (1997) ; Lefebvre et al. (2000)	Montech Landfill (near Toulouse, France)	43.96N, 1.23E[c]	Temperate, no dry season, warm summer	*13.6*	*454*	20	0 to 2
Koerner (2001)	(near Philadelphia, Pennsylvania, USA)	40.65N, 75.43W	Cold, no dry season, warm summer	*10.6*	*1156*	50	0 to 8
Yoshida and Rowe (2003)	Tokyo Port Landfill (Tokyo, Japan)	35.62N, 139.78E[d]	Temperate, no dry season, hot summer	*16.1*	*1406*	35	7 to 20
Hanson et al. (2010)	Sauk Trail Hills Landfill (Canton, Michigan, USA)	42.27N, 83.46W	Cold, no dry season, warm summer	9.8	835	31.3	0 to 13
Hanson et al. (2010)	Los Corralitos Regional Landfill (Las Cruces, New Mexico, USA)	32.33N, 106.77W	Arid, steppe, cold	18.2	240	19	3 to 12
Hanson et al. (2010)	Anchorage Regional Landfill (Anchorage, Alaska, USA)	61.24N, 149.86W	Cold, no dry season, cold summer	2.3	408	60	6 to 15.6
Hanson et al. (2010)	Vancouver Landfill (Delta, British Columbia, Canada)	49.11N, 123.00W	Temperate, no dry season, warm summer	9.9	1167	19	0 to 33
Bouazza et al. (2011)	(Southeast of Melbourne, Australia)	38.13S, 145.35E[e]	Temperate, no dry season, warm summer	*15.8*	*553*	8	0 to 1.5
Bonany et al. (2013)	(Ste. Sophie, Quebec, Canada)	45.82N, 73.90W	Cold, no dry season, warm summer	*6.7*	*997*	25	0 to 2.5
NP	Santa Maria Regional Landfill (Santa Maria, California, USA)	34.95N, 120.38W	Temperate, dry, warm summer	8.7[f]	354[f]	19	1.7 to 7.3
NP	Cold Canyon Landfill (San Luis Obispo, California, USA)	35.19N, 120.60W	Temperate, dry, warm summer	8.7[f]	354[f]	33.5	0 to 17

Italicized numbers in the average annual temperature and average annual precipitation columns indicate data was obtained from http://www.msn.com/en-gb/weather/records/.
NP – Not previously published.
[a] From Koppen–Geiger Climate Classification System (Peel et al., 2007).
[b] Coordinates for Chelmsford, Essex, UK.
[c] Coordinates for Montech, France.
[d] Coordinates for Tokyo Port.
[e] Coordinates near Cranbourne, Australia.
[f] From NOAA.
[g] Total depth of waste at sensor location.

approximately 2.3 mm/day for MSW heat generation (Yesiller et al., 2005). Temperatures at time of placement affected the waste temperatures developing over time. Wastes placed at temperatures of 15–20 °C resulted in stable temperatures ranging from 25 to 55 °C after 2 years (Fig. 1a). Below freezing (i.e., <0 °C) temperatures at time of placement had particularly significant long-term effects on heat generation in MSW landfills. Wastes frozen at time of placement remained frozen for extended periods of time, on the order of 1–2 years in MSW landfills in cold regions due to latent heat effects, insulative qualities of MSW, and overall cold climatic conditions. In temperate climates, combined high waste temperatures at time of placement (generally corresponding to seasonal high air temperatures) and high precipitation resulted in the highest temperatures, whereas in cold regions, high waste temperatures at time of placement and optimum precipitation resulted in high temperatures.

Temperature data for a MSW landfill in Ohio, USA containing significant amount of aluminum processing waste have been reported (Stark et al., 2012; Jafari et al., 2014). Temperatures up to 100–150 °C were reported for the site. This site was not analyzed in detail herein due to lack of detailed temperature versus depth or time data; disposal conditions at the site with the significant amount of aluminum wastes not representing typical MSW landfill conditions; and temperatures having been measured in open conduits.

Time rates of temperature variation in wastes (expressed in °C/yr with positive values indicating increase) are presented in Fig. 2 as a function of time. An inverse relationship was observed between rate of temperature change and time, where rate of temperature change decreased with time. High rates of temperature increases, in excess of 40 °C/yr, were observed in fresh (i.e., young) wastes; whereas low rates of temperature variation, on the order of −1 to 3 °C/yr, were observed in old wastes. The temperature increases in wastes over time in cold climates were generally lower than the waste temperature increases over time in temperate climates. The rate of thawing of frozen wastes, which included phase change and latent heat requirements, was low and on the order of 1 °C/yr.

Variation of waste temperatures with depth is presented in Fig. 3 for waste ages varying from 0 to over 20 years. Temperature envelopes showing limiting high and low temperature profiles are included in the figure. Normalized depth was used in the figure, where 0 and 1.0 corresponded to elevations of top surface and bottom liner/subgrade at a given site, respectively. This normalized depth representation was used throughout the paper. The highest temperatures typically were observed at central locations within the waste masses. Temperatures at near-surface locations typically were lower than the maximum values and influenced by seasonal air temperature variations. Temperatures near the base of the landfills typically were lower than the maximum

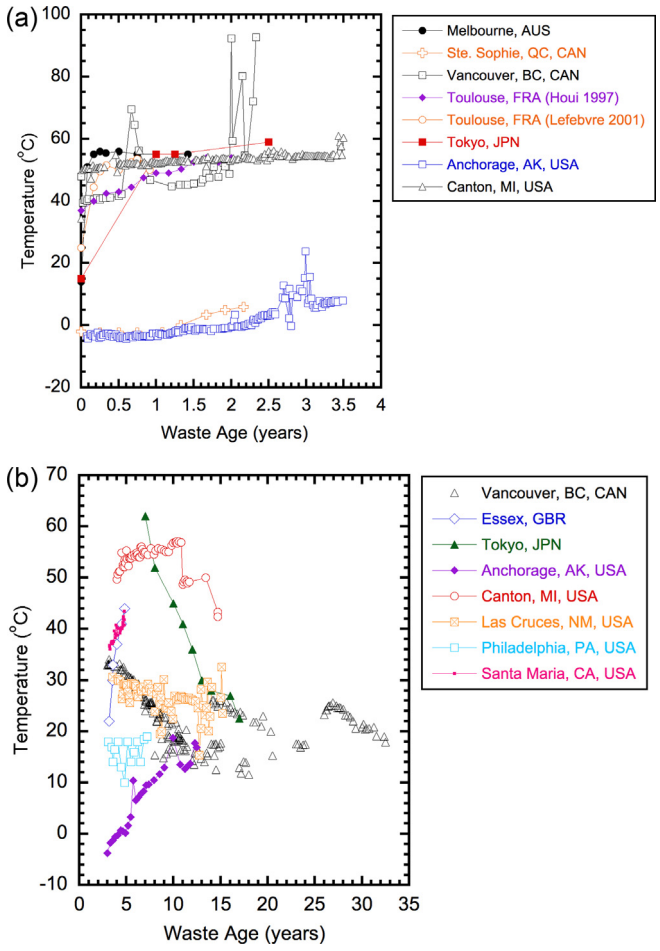

Fig. 1. Variation of MSW temperatures with time (a) young wastes (age < 3.5 years) and (b) old wastes (age 3–33 years).

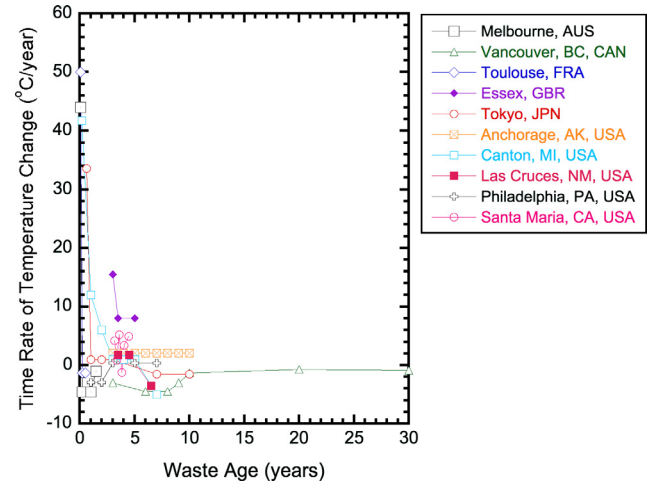

Fig. 2. Time rate of temperature change for MSW.

values at central locations, yet elevated in comparison to mean annual earth temperature at the sites. The curvature of the temperature–depth relationships generally diminished over time with more linear relationships observed for old wastes than young wastes. Maximum stable temperatures measured for MSW are summarized in Table 2.

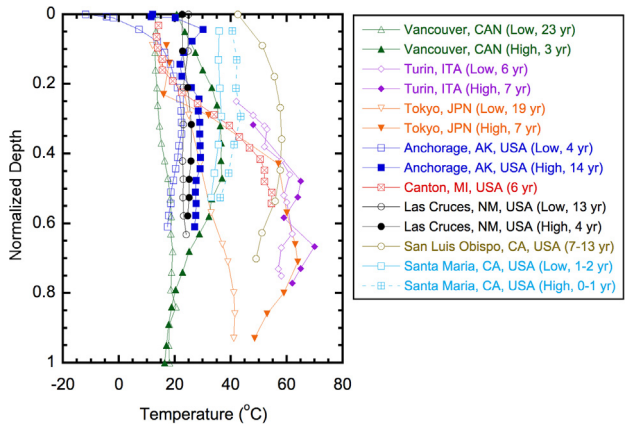

Fig. 3. Variation of MSW temperatures with depth.

Thermal gradients (i_t) were calculated for zones above and below the elevation of maximum temperature using temperature–depth relationships available at the sites included in the study as: $(T_{distal} - T_{proximal})/z$, where $T_{proximal}$ and T_{distal} = temperature closer to and farther from the ground surface, respectively and z = vertical distance between the locations used for temperature. Using this definition, positive i_t represented upward heat flow, which generally prevailed at shallow depths (above elevations of maximum temperatures), whereas negative i_t represented downward heat flow, which generally prevailed at depths below the location of maximum temperatures. This definition for thermal gradient and corresponding sign convention were used throughout the paper. The thermal gradients calculated for the MSW sites included in the study are presented in Table 2. The thermal gradients for MSW ranged between approximately −13.1 and +16.1 °C/m (Table 2). For approximately 60% of the cases included in Table 2, the absolute magnitudes of the shallow zone gradients were higher than the deep zone gradients indicating more prominent upward heat flow toward the ground surface than downward heat flow toward the subsurface.

Schematics of expected trends for MSW temperature variation with depth are presented in Fig. 4 for typical landfilling conditions (Fig. 4a) and for vertical landfill expansions (Fig. 4b). The vertical temperature profile trend lines for typical conditions were drawn based on data presented in this paper and for the case of vertical landfill expansions based on data from Yesiller et al. (2011). At sites with relatively high heat generation and low mean annual earth temperature, the highest waste temperatures occurred at central depths with a generally convex shape of temperature–depth relationship and a large difference between maximum and minimum temperatures with depth. The curvature of the temperature–depth relationship was low at sites with relatively low heat generation and high mean annual earth temperature with a nearly uniform temperature–depth relationship and a corresponding low difference between maximum and minimum temperatures throughout the depth of the waste mass. Also, curvature of temperature–depth relationships was low for old wastes in comparison to recently placed wastes (Fig. 4a). The addition of significant amount of fresh wastes to existing wastes due to vertical expansion at a facility resulted in an upward shift and increase in the overall thickness of the elevated temperature zone and the formation of a new temperature profile (Fig. 4b).

2.2. MSW incinerator ash temperatures

Data on MSW incinerator ash temperatures was limited in comparison to MSW and mining waste temperature data. Temperature

Table 2
MSW temperatures and thermal gradients.

Source	Site/location	Peak temperature (°C)	Peak temperature location (normalized depth)	Waste age at peak temperature (years)	Shallow zone thermal gradient (°C/m)	Deep zone thermal gradient (°C/m)
Rees (1980a)	Aveley Landfill (near Essex, UK)	45	0.38	3 to 6	16.07	−13.12
Zanetti et al. (1997)	(Turin, Italy)	70	0.67	7	2.62	−3.33
Houi et al. (1997)	Montech Landfill (near Toulouse, France)	58	0.65	0 to 2	1.5	−2.6
Lefebvre et al. (2000)	Montech Landfill (near Toulouse, France)	62	0.45	0 to 1	6.05	0
Koerner (2001)	(near Philadelphia, Pennsylvania, USA)	30	0.6	1	0.53	−0.95
Yoshida and Rowe (2003)	Tokyo Port Landfill (Tokyo, Japan)	64	0.71	7.2	1.90	−0.87
NP	Sauk Trail Hills Landfill (Canton, Michigan, USA)	62	0.54	3.5	2.54	−3.08
Hanson et al. (2010)	Los Corralitos Regional Landfill (Las Cruces, New Mexico, USA)	30	0.47	4	1.39	−0.46
Hanson et al. (2010)	Anchorage Regional Landfill (Anchorage, Alaska, USA)	55	0.6	10	0.81	−1.08
NP	Vancouver Landfill (Delta, British Columbia, Canada)	92	0.5	2	1.37	−1.32
Bouazza et al. (2011)	(Southeast of Melbourne, Australia)	65	0.5	0.2	15	−11.95
Bonany et al. (2013)	(Ste. Sophie, Quebec, Canada)	4	0.56	2	2.3	−1.4
NP	Santa Maria Regional Landfill (Santa Maria, California, USA)[a]	44	0.28	3.2	1.53	−2.3
NP	Cold Canyon Landfill (San Luis Obispo, California, USA)	58	0.36	3	1.31	−0.79

NP – Not previously published.
[a] 6.5 m of earthen embankment covered waste, depths measured from top of waste layer.

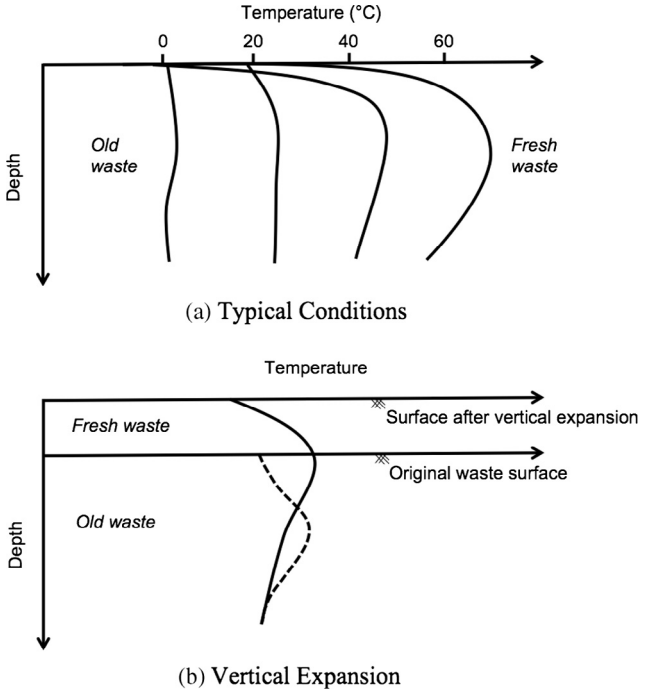

Fig. 4. Schematic temperature profiles for MSW.

data were presented for a site located in Ingolstadt, Germany (48.76N, 11.41W) with a temperate climate (no dry season, warm summer, Koppen–Geiger Climate Zone (Peel et al., 2007)) and 15 °C average annual air temperature and between 800 and 1000 mm annual precipitation for the reported study period (Klein et al., 2001). Data were provided for an area with a waste mass depth of 10 m and waste age of 2–3 years. A leachate collection and removal system was used at the site, whereas active gas collection was not present. The ash waste at the landfill was not covered during the temperature data collection period. The waste temperatures increased upon placement with the peak temperature for the ash waste measured to be 87 °C at a normalized depth of 0.4 three months subsequent to placement. Temperatures two to three years subsequent to placement were generally stable in the range of approximately 45–55 °C with slightly decreasing trends. The waste temperatures at shallow depths (i.e., near ground surface) of the landfill were affected by outside air temperature and fluctuated seasonally. The lowest measured temperature in the ash landfill was approximately 5 °C. The shallow zone and deep zone thermal gradients within the waste mass were +23.3 and −8.8 °C/m, respectively.

2.3. Mining waste temperatures

A summary of the location, climatic conditions, and site details for the mining waste disposal sites included in the paper are provided in Table 3. The majority of the mining wastes included waste rock piles with data from one site with mine tailings. Waste rocks consist of material extracted typically from open mine pits to access underlying ore and have a wide range of sizes (sub-millimeters to tens of centimeters to over a meter) with the majority in the coarse grained soil sizes range according to the USCS, whereas mine tailings are generated as a byproduct of ore treatment and typically have sand and silt size particles (Lefebvre et al., 1997). The waste rocks included in this review typically were well graded with sizes ranging from less than 2 mm to over 150 mm (Lefebvre et al., 1997; Lefebvre et al., 2001; Hollesen et al., 2009; Nunoo, 2009; Smith et al., 2013; Lahmira et al., 2014). The mine tailings at the Huelva, Spain site had sizes ranging from silt to fine–medium sand (Blanco et al., 2013). Peripheral and underlying drainage

Table 3
Site description: mining waste.

Source	Type of waste	Site/location	Latitude and longitude	Climatic region[a]	Average annual air temperature (°C)	Average annual precipitation (mm)	Pile dimensions	Waste rock/tailings type, Pyrite mass fraction [%]	Waste age (years)
Harries and Ritchie (1981)	Uranium Mining Waste	Rum Jungle (Batchelor, Northern Territory, Australia)	12.98S, 131.02E	Tropical savannah	27.4	1500	13 to 18 m high	Carbonaceous slates, graphitic schists [3]	20
Lefebvre et al. (1997, 2001), Sracek et al. (2004), Da Silva et al. (2009)	Gold Mining Waste	Doyon Mine (Rouyn-Noranda, Quebec, Canada)	48.37N, 78.55W	Cold, no dry season, warm summer	2.0	864	500 × 900 m, 30 to 35 m high	Sericite schists, dioritic rocks [1.5 to 7]	9 to 14
Lefebvre et al. (2001)	Uranium Mining Waste	Nordhalde Waste Pile (Ronnenberg Mining District, Thuringia, Germany)	50.90N, 12.08E[b]	Cold, no dry season, warm summer	8.3	562	800 × 1450 m, 80 m high	Slate [1 to 2]	30
Wels et al. (2003)	Molybdenum Mine Waste	(Questa, New Mexico, USA)	36.71N, 105.59W	Arid, steppe, cold	9.2	333	30 to 60 m high	Mixed volcanics [3.5]	19 to 37
Hollesen et al. (2009)	Coal Mining Waste	(Svalbard, Norway)	78.75N, 15.97E	Polar tundra	−5.8	187	22 m high	Sandstone, siltstone, conglomerate, schist [<1]	20
Lahmira et al. (2014)	Coke from Oil Sands Mine	(Calgary, Alberta, Canada)	51.08N, 114.08W	Cold, no dry season, warm summer	2.0	439	5:1 and 3:1 (horizontal:vertical) slopes, 33 m high	Coke [–]	4
Pham et al. (2013)	Diamond Mining Waste	Diavik Diamond Mine (Yellowknife, Northwest Territories, Canada)	62.46N, 114.37W	Cold, no dry season, cold summer	−8.9	280	50 × 60 m, 15 m high	Granite with small amounts of sulfide-bearing biotite schist [>0.08]	0 to 2.5
Blanco et al. (2013)	Mine Tailings	Monte Romero Mine (Huelva, Spain)	37.53N, 6.92W	Temperate, dry summer, hot summer	19.5	1000	2 to 4 m high	Sulfides and silicates [12]	28

[a] From Koppen–Geiger Climate Classification System (Peel et al., 2007).
[b] Coordinates for Gera, Germany.

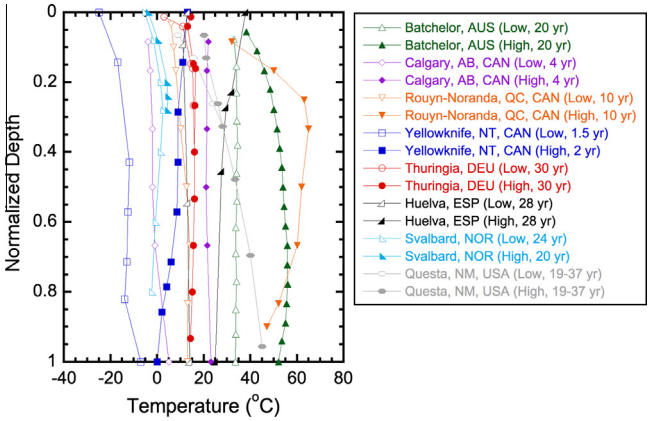

Fig. 5. Variation of mining waste temperatures with depth.

systems typically were installed to collect surface runoff and leachate. Gas collection systems typically were not used at the mining waste disposal sites. The mining wastes included in the analysis were generally uncovered except for the site in Alberta (Canada), which had a soil cover system with a thickness of approximately 0.6–1.1 m and the site in Germany, which was indicated to have a soil cover of variable thickness.

Variations of mining waste temperatures with depth are presented in Fig. 5. Maximum stable temperatures measured in mining wastes and thermal gradients measured for temperature–depth profiles available at the sites included in the study are summarized in Table 4. Mining waste temperatures in the range of −25 to 65 °C were reported in the literature (Fig. 5). The highest mining waste temperatures at depth were in the range of 30–65 °C and were measured in Northern Territory (Australia), Quebec (Canada), and New Mexico (USA). Elevated temperatures were present for timeframes in excess of decades. Temperature variations less than 1 to over 30 °C were measured with depth in mine waste piles (Fig. 5). In general, less spatial and temporal variations were observed in mining waste temperatures than MSW temperatures. The thermal gradients within the waste piles ranged from −9.4 to +5.0 °C/m (Table 4). In almost all of the cases included in Table 4, the absolute magnitude of the shallow zone gradients were higher than the deep zone gradients indicating more prominent upward heat flow toward the surface in the mining waste piles than downward heat flow toward the subsurface.

Table 4
Mining waste temperatures and thermal gradients.

Source	Site/location	Peak temperature (°C)	Peak temperature location (normalized depth)	Waste age at peak temperature (years)	Shallow zone thermal gradient (°C/m)	Deep zone thermal gradient (°C/m)
Harries and Ritchie (1981)	Rum Jungle (Batchelor, Northern Territory, Australia)	56	0.7	20	1.83	−0.52
Lefebvre et al. (1997)	Doyon Mine (Rouyn-Noranda, Quebec, Canada)	65	0.5	10	2.6	−0.5
Lefebvre et al. (2001)	Doyon Mine (Rouyn-Noranda, Quebec, Canada)	50	0.4	9	3.16	−1.41[a]
Sracek et al. (2004)	Doyon Mine (Rouyn-Noranda, Quebec, Canada)	60	0.5	14	4.13	−0.27
Da Silva et al. (2009)	Doyon Mine (Rouyn-Noranda, Quebec, Canada)	65	0.5	13.5	3	−1.87
Lefebvre et al. (2001)	Nordhalde Waste Pile (Ronnenberg Mining District, Thuringia, Germany)	16	0.2	30	0.57	−0.03[a]
Wels et al. (2003)	(Questa, New Mexico, USA)	45.5	0.51	19 to 37	1.88	NA
Hollesen et al. (2009)	(Svalbard, Norway)	37	0.36	20	1.23	−0.32
Lahmira et al. (2014)	(Calgary, Alberta, Canada)	50	0.8	4	0.9	−3.3[a]
Pham et al. (2013)	Diavik Diamond Mine (Yellowknife, Northwest Territories, Canada)	10	0.07	0 to 2.25	2.17	−0.45
Blanco et al. (2013)	Monte Romero Mine (Huelva, Spain)	26	0.33	28	−9.4 to 5	−0.77

NA – Not applicable.
[a] Assuming 10 m below the pile base is at mean annual earth temperature.

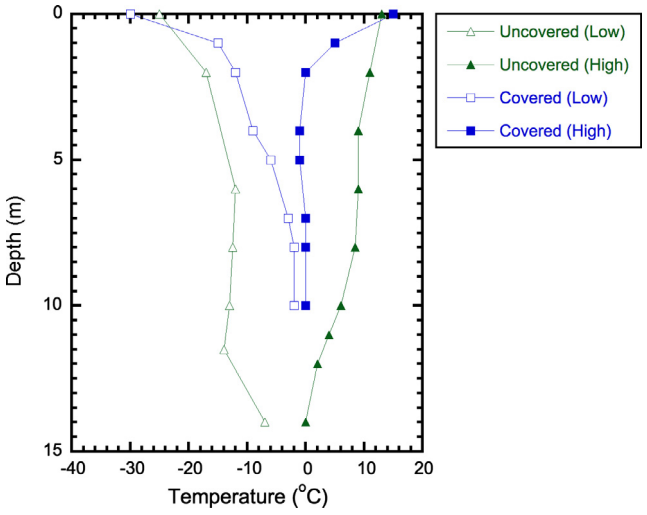

Fig. 6. Mining waste temperatures for uncovered and covered (bottom of the cover: 4 m) conditions.

The time versus temperature and depth versus temperature relationships were generally linear with slight increasing or decreasing trends with the exception of the sites located in Quebec (Canada) and New Mexico (USA). The temperature profiles at these two sites exhibited similarities to the profiles observed for MSW (e.g., Figs. 3 and 4a). The Quebec site with the relatively colder subgrade temperature exhibited a convex temperature versus depth relationship, whereas the New Mexico site with the relatively higher subgrade temperature exhibited an increasing temperature with depth trend. The maximum mining waste temperatures were observed in Quebec with an average precipitation of 2.4 mm/day in similarity to the maximum temperatures observed for MSW at the Michigan (USA) site with an average precipitation of 2.3 mm/day. The mining waste temperatures were relatively low and uniform at sites with cold and dry climates (Fig. 5 and Table 3).

Additional analysis was conducted for the site in Northwest Territories (Canada) by comparing temperature versus depth relationships from two waste piles as presented in Fig. 6. Data were obtained at the site from a pile with uncovered waste (Tables 3 and 4 and Fig. 5) and also a pile with a two-layer cover system (2 m non-reactive waste rock with low pyrite content underlain by 2 m till) (Pham et al., 2011). The physical characteristics and age of the mining wastes in the uncovered and covered piles were similar. The range of temperatures at a given depth was lower (i.e., higher minimum and lower maximum temperatures) in the covered waste pile than the uncovered waste pile (Fig. 6). The low permeability till layer reduced infiltration of moisture and oxygen into the waste rock mass decreasing the extent of the biochemical reactions. In addition, the high permeability rock layer at the surface provided natural convection reducing temperatures in winter (Pham et al., 2011). The waste rock temperatures in the covered pile remained below 0 °C throughout the year, whereas above freezing temperatures occurred in the uncovered waste rock pile (Fig. 6).

Pyrite mass fraction of the mining wastes in most cases was observed to be related to the maximum temperatures measured in the wastes (Tables 3 and 4). Heat generation in mining wastes mainly results from biologically aided exothermic reactions between pyrite and oxygen and water. In general, high temperatures were observed for sites with high pyrite fraction in the mining waste mass.

3. Waste thermal properties

Thermal properties including thermal conductivity (k_t), volumetric heat capacity (c), and thermal diffusivity (α) reported for MSW and mining wastes are presented in Tables 5 and 6, respectively. The thermal conductivity of MSW varied by more than 30× from 0.044 to 1.5 W/m K. The thermal conductivity of mining wastes was higher (from 0.35 to 3.5 W/m K) with less variation in k_t values between the different studies included in Table 6. The volumetric heat capacity and thermal diffusivity also were higher for mining waste than MSW. The volumetric heat capacity varied between 378 and 4000 kJ/m^3 K and 838 and 2933 kJ/m^3 K for

Table 5
Thermal properties of waste: MSW.

Source	Composition	Site/location	Density (kg/m^3)	Thermal conductivity (W/m K)	Specific heat (kJ/m^3 K)	Thermal diffusivity (m^2/s)
Zanetti et al. (1997)	Organic/Garden: 47.3–57% Wood: 21.4–26.1% Plastic: 8.6–9% Other: 12.6–18%	(Turin, Italy)	600 (initial), 1000 (10-year old)	0.0445	1302 to 2170	3.4×10^{-8} (initial), 2.1×10^{-8} (10-year old)
Hanson et al. (2000); NP	NA	Sauk Trail Hills Landfill (Canton, Michigan, USA)	1000	0.1 to 0.7	800 to 4000	2.5×10^{-8} to 8.8×10^{-7}
Lefebvre et al. (2000)	Municipal: 63.4% Incinerated: 21.4% Bottom Ash: 2.4% Sludge: 1.8% Produce: 1.1% Yard: 8.8% Bulky Refuse: 1.2%	Montech Landfill (near Toulouse, France)	600 to 950	0.1	378 to 950	1.5×10^{-7}
Yoshida et al. (1997), Yoshida and Rowe (2003)	Fresh Wastes Paper and Textile: 28.4% Plastics and Rubber: 15.4% Wood: 5.9% Food: 19.4% Incombustibles and Others: 30.9% Older Wastes (2–5 years after landfilling) Paper and Textile: 6.0% Plastics and Rubber: 17.2% Wood: 5.2% Food: 0% Incombustibles and Others: 71.6%	Tokyo Port Landfill (Tokyo, Japan)	Unsaturated: 1157, Saturated: 1424	Unsaturated: 0.35, Saturated: 0.96	Unsaturated: 2198, Saturated: 3418	Unsaturated: 1.6×10^{-7}, Saturated: 2.8×10^{-7}
Hanson et al. (2006)	NA	Anchorage Regional Landfill (Anchorage, Alaska, USA)	530	0.23	742	3.2×10^{-7}
Hanson et al. (2008)	NA	Sauk Trail Hills Landfill (Canton, Michigan, USA)	1000	1.0	2000	5×10^{-7}
Hanson et al. (2008)	NA	Los Corralitos Regional Landfill (Las Cruces, New Mexico, USA)	750	0.6	1200	5×10^{-7}
Hanson et al. (2008)	NA	Anchorage Regional Landfill (Anchorage, Alaska, USA)	530	0.3	1000	3×10^{-7}
Hanson et al. (2008)	NA	Vancouver Landfill (Delta, British Columbia, Canada)	1000	1.5	2200	5×10^{-7}
Zambra and Moraga (2013)	NA	Modeling Study	575	0.18 (cellulose)	1909	9.4×10^{-8}
Bonany et al. (2013)	Frozen Waste Unfrozen Waste	(Ste. Sophie, Quebec, Canada)	930	$T \leqslant 0$: 0.45 $T > 0$: 0.45 + 0.025T	930	4.8×10^{-7}

NA – Not available.
NP – Not previously published.

MSW and mining waste, respectively. The thermal diffusivity varied from 2.1×10^{-8} to 8.8×10^{-7} m^2/s and from 1.2×10^{-7} to 1.5×10^{-6} m^2/s for MSW and mining waste, respectively. The data reported for ash waste included intermediate values between MSW and mining wastes: $k_t = 0.7$ W/m K, $c = 1704$ kJ/m^3 K, and $\alpha = 4.1 \times 10^{-7}$ m^2/s (Klein et al., 2003).

4. Average temperature differential

The average temperature differential (ΔT_{avg}) in the wastes was calculated to assess heat generation potential of a given waste mass. The average temperature differential represents the time-averaged temperature rise above ambient (i.e., unheated) waste conditions (Hanson et al., 2010). The average temperature differential was calculated as the average difference between the measured waste temperature and the baseline unheated waste temperature at a given depth. The waste temperatures were obtained from measured data provided in the studies included in this paper. The baseline unheated temperature included the temperature of the waste under the influence of only seasonal ground temperature fluctuations (and did not include any heat generation). The baseline temperature was calculated using conventional near-surface earth temperature theory as presented in Eq. (1) (ORNL, 1981).

Table 6
Thermal properties of waste: mining waste.

Source	Type of waste Compositional details	Site/location	Density (kg/m^3)	Thermal conductivity (W/m K)	Specific heat (kJ/m^3 K)	Thermal diffusivity (m^2/s)
Harries and Ritchie (1981)	Uranium Mining Waste Volumetric Water Content (Wet Season): 0.12 Volumetric Water Content (Dry Season): 0.05	Rum Jungle (Batchelor, Northern Territory, Australia)	1670	NA	1446	6.8×10^{-7} (Wet Season), 4.9×10^{-7} (Dry Season)
Blackford and Harries (1985)	Uranium Mining Waste	Rum Jungle (Batchelor, Northern Territory, Australia)	NA	1.8 to 3.1	NA	NA
Tan and Ritchie (1997)	Copper Mine	Aitik Mine (Sweden)	NA	0.7 to 1.6	NA	NA
Bennett et al. (1995)	Base Metal (Copper, Lead, Zinc) Mining Waste	Heath Steele Mine (New Brunswick, Canada)	NA	1 to 1.2	NA	NA
Lefebvre et al. (1997)	Gold Mining Waste Water Saturation: 0.32 Porosity: 0.33	Doyon Mine (Rouyn-Noranda, Quebec, Canada)	1840	2.22 to 2.92	1980	1.2×10^{-7} to 1.5×10^{-6}
Tan and Ritchie (1997)	Gold Mining Waste	Kelian Gold Mine (Kalimantan, Indonesia)	NA	1.6 to 3.3	NA	NA
Lefebvre et al. (2001)	Gold Mining Waste Water Saturation: 0.42 Porosity: 0.33	Doyon Mine (Rouyn-Noranda, Quebec, Canada)	1950	2.5	2933	1.5×10^{-6}
Lefebvre et al. (2001)	Uranium Mining Waste Water Saturation: 0.63 Porosity: 0.3	Nordhalde Waste Pile (Ronnenberg Mining District, Thuringia, Germany)	2114	1	2158	6.7×10^{-7}
Sracek et al. (2004)	Gold Mining Waste Total SO_4^{2-}: 2.8–4.6% by weight Inter-block porosity: 0.33 Intra-block porosity: 0.05	Doyon Mine (Rouyn-Noranda, Quebec, Canada)	1836	NA	NA	NA
Smith and Glasser (2005)	Lignite to Anthracite	Laboratory Setting	NA	NA	1500 to 2100	NA
Hollesen et al. (2009)	Coal Mining Waste	(Svalbard, Norway)	NA	0.7	2000	3.5×10^{-7}
Lahmira et al. (2014)	Coke (90% carbon)	(Calgary, Alberta, Canada)	NA	Dry: 0.35 Wet: 0.8 At Mean Saturation: 0.88	838	1.1×10^{-6}[a]
Pham et al. (2011, 2013)	Diamond Mining Waste	Diavik Diamond Mine (Yellowknife, Northwest Territories, Canada)	NA	1.3–3.5	2130 (for thermal conductivity of 1.65 W/m K)	NA

NA – Not available.
[a] Assuming density = 1900 kg/m^3 (approximate average for values reported in other papers listed herein).

$$T_{(x,t)} = T_m - A_s e^{-x\sqrt{\pi/365\alpha}} \cos\left[\frac{2\pi}{365}\left(t - t_0 - \frac{x}{2}\sqrt{\frac{365}{\pi\alpha}}\right)\right] \quad (1)$$

where $T_{(x,t)}$ is temperature (°C) at depth x and time t, T_m is mean annual earth temperature (°C), A_s is amplitude of annual surface temperature wave (°C), x is the depth below the surface (m), α is thermal diffusivity (m^2/day), t is time of year (days, 0 = midnight December 31), and t_0 is a phase constant (34.6 days). In calculation of baseline unheated temperatures, site-specific thermal diffusivity values (α) for wastes were used (Tables 5 and 6). For sites where no thermal diffusivity data was reported, the α for a region of similar climatic conditions (i.e., temperature and precipitation) was used.

The average temperature differential varied over time due to combined temporal fluctuations of the measured waste temperatures and baseline unheated temperatures. To provide a representative value, the temperature differential was calculated over the period of measurements available as the area between the time–temperature curves for measured waste and calculated unheated conditions divided by the duration of the analysis period, resulting in units of °C-day/day. ΔT_{avg} data were generated for each measurement depth at a given site. The peak ΔT_{avg} (representing maximum stable temperatures measured at a given site) typically was observed at central depths of the waste mass. The peak average temperature differentials ($\Delta T_{avg\text{-}peak}$) determined for all of the sites (MSW, incinerator ash, and mining waste) included in the study are summarized in Table 7. The $\Delta T_{avg\text{-}peak}$ ranged from 3.4 to 41.6 °C-day/day for MSW, was 49.7 °C-day/day for MSW incinerator ash, and ranged from 0.4 to 38.4 °C-day/day for mining waste (Table 7). For the MSW landfill in Quebec, Canada, the $\Delta T_{avg\text{-}peak}$ was negative, indicating that the measured waste temperatures were below the baseline unheated waste temperatures for the monitoring period reported.

To provide comparison between the sites included in the study with different data collection periods, peak average temperature differential for the sites was calculated using the maximum stable elevated temperatures measured at a given site over a period of 1 year (Table 7). The one-year peak average temperature differential ($\Delta T_{avg\text{-}peak\text{-}one\ year}$) was determined for the same depth as $\Delta T_{avg\text{-}peak}$

Table 7
Average temperature differential: MSW, MSW ash, and mining waste.

Source	Type of waste	Site/location	Peak average temperature differential (°C/day/day)	One-year peak average temperature differential (°C/day/day)	Waste age (years)
Rees (1980a)	MSW	Aveley Landfill (near Essex, UK)	22.6	31.7	3 to 5
Houi et al. (1997)	MSW	Montech Landfill (near Toulouse, France)	30.0	40.5	0 to 2
Lefebvre et al. (2000)	MSW	Montech Landfill (near Toulouse, France)	30.6	44.6	0 to 1
Koerner (2001)	MSW	(near Philadelphia Pennsylvania, USA)	3.4	15.9	0 to 7
Yoshida and Rowe (2003)	MSW	Tokyo Port Landfill (Tokyo, Japan)	17.8	44.1	7 to 17
Hanson et al. (2008)	MSW	Sauk Trail Hills Landfill (Canton, Michigan, USA)	41.6	42.7	4 to 11
Hanson et al. (2008)	MSW	Los Corralitos Regional Landfill (Las Cruces, New Mexico, USA)	6.1	9.1	0 to 13
Hanson et al. (2008)	MSW	Anchorage Regional Landfill (Anchorage, Alaska, USA)	32.2	49.2	8 to 16
Hanson et al. (2008)	MSW	Vancouver Landfill (Delta, British Columbia, Canada)	11.1	49.1	3 to 13
Bouazza et al. (2011)	MSW	(Southeast of Melbourne, Australia)	35.5	46.7	0 to 1.5
Bonany et al. (2013)	MSW	(Ste. Sophie, Quebec, Canada)	−9.3	−8.5	0 to 2
NP	MSW	Santa Maria Regional Landfill (Santa Maria, California, USA)	20.3	25.2	3 to 5
NP	MSW	Cold Canyon Landfill (San Luis Obispo, California, USA)	32.1	44.5	0 to 17
Klein et al. (2001, 2003)	MSW Ash	(Ingolstadt, Germany)	49.7	75.9	0 to 3
Harries and Ritchie (1981)	Uranium Mining Waste	Rum Jungle (Batchelor, Northern Territory, Australia)	25.8	25.8[a]	20
Lefebvre et al. (1997)	Gold Mining Waste	Doyon Mine (Rouyn-Noranda, Quebec, Canada)	38.4	39.0	0 to 2
Lefebvre et al. (2001)	Gold Mining Waste	Doyon Mine (Rouyn-Noranda, Quebec, Canada)	22.0	31.3	0 to 15
Lefebvre et al. (2001)	Uranium Mining Waste	Nordhalde Waste Pile (Ronnenberg Mining District, Thuringia, Germany)	0.4	1.7	0 to 25
Hollesen et al. (2009)	Coal Mining Waste	(Svalbard, Norway)	6.1	8.5	20 to 22
Pham et al. (2013)	Diamond Mining Waste	Diavik Diamond Mine (Yellowknife, Northwest Territories, Canada)	2.3	3.2	1 to 2
Blanco et al. (2013)	Mine Tailings	Monte Romero Mine (Huelva, Spain)	5.3	5.3	28

NP – Not previously published.
[a] Peak value for one measurement in time assumed to remain constant for a one-year period.

and ranged from 9.1 to 49.2 °C-day/day for MSW, was 75.9 °C-day/day for MSW incinerator ash, and ranged from 1.7 to 39.0 °C-day/day for mining waste (Table 7). $\Delta T_{avg\text{-}peak\text{-}one\ year}$, in similarity to $\Delta T_{avg\text{-}peak}$, was negative for the MSW landfill located in Quebec. In general, $\Delta T_{avg\text{-}peak\text{-}one\ year}$ was greater than $\Delta T_{avg\text{-}peak}$. The differences were most pronounced for wastes that had undergone large time rates of temperature change, whereas less difference was observed for sites with relatively stable temperature trends.

$\Delta T_{avg\text{-}peak}$ was correlated to average annual precipitation to further investigate the influence of moisture conditions on elevated temperatures in wastes (Fig. 7). In general, the maximum peak average temperature differential was observed for intermediate levels of annual precipitation. $\Delta T_{avg\text{-}peak}$ increased with increasing precipitation up to an optimum level, beyond which the temperature differential decreased with further increases in precipitation. This observation was consistent with previous findings for MSW (Yesiller et al., 2005). The bell-shaped $\Delta T_{avg\text{-}peak}$ versus average annual precipitation relationship was observed for both MSW and mining wastes (Fig. 7). The biological and chemical reactions occurring in the wastes were enhanced with increasing precipitation and associated higher moisture content of the wastes. However, increasingly higher heat capacity of wastes resulting from higher moisture contents associated with increasing precipitation required relatively large energy inputs for heat gain, preventing further rise in waste temperatures at high levels of precipitation beyond optimum conditions.

5. Waste heat generation

The average temperature differential values were used together with site-specific thermal properties and representative site-specific boundary conditions to determine heat generation in wastes. Heat generation values at the MSW landfills, the mining waste piles, and the MSW incinerator ash landfill included in this review were estimated using the approach provided in Yesiller et al. (2005). At each site, heat generation was determined for wastes that had reached maximum stable temperatures, which were typically located near the central core of the waste mass.

The waste heat generation is dependent on the magnitude of temperature increase of the waste from biochemical reactions, the heat capacity of the waste, and the heat losses to the surrounding environment. The thermal energy produced, which was used to heat the waste mass was calculated as:

$$E_{heating} = \sum_{i=1}^{n} \Delta T_i c \qquad (2)$$

where $E_{heating}$ is energy used to heat waste (MJ/m^3), ΔT_i is increment of temperature rise for waste (K), and c is volumetric heat capacity of waste (MJ/m^3 K).

The $E_{heating}$ represented heat energy required to raise the temperature of a given volume of waste by an amount equal to the peak average temperature differential. The peak average temperature differential ($\Delta T_{avg\text{-}peak}$, Table 7) for a given site was used as the total amount of temperature increase ($\Sigma \Delta T_i$) for the waste at the site. The volumetric heat capacity values provided in Section 3 were used for MSW, mining wastes, and MSW incinerator ash. The energy produced used for heating waste describes a one-time heat gain and is reported in units of MJ/m^3. The results of the heat generation analyses for MSW and mining wastes are presented in Tables 8 and 9, respectively. $E_{heating}$ in MSW ranged from −8.6 to 83.1 MJ/m^3 (negative value indicating a deficit of heat energy as compared to baseline unheated waste conditions), whereas the

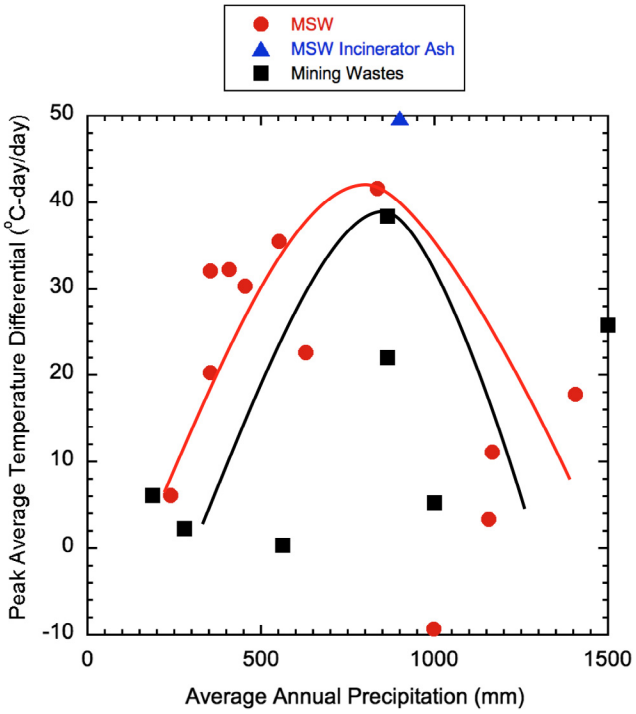

Fig. 7. Variation of $\Delta T_{avg\text{-}peak}$ with annual precipitation.

range of heat generated and used for heating mining wastes was 0.6–72.6 MJ/m^3. The $E_{heating}$ for the MSW incinerator ash landfill in Germany was 72.6 MJ/m^3.

Thermal losses were determined using one-dimensional (i.e., vertical) conductive heat transfer analysis on a site-specific basis with reference to the waste temperature profiles with depth. The heat fluxes associated with thermal losses were calculated as the product of thermal conductivity (k_t, from Section 3) and thermal gradient (i_t, from Section 2). For sites where thermal conductivity of waste was not reported, k_t values for wastes for a region of similar climatic conditions (i.e., temperature and precipitation) were used. Losses were calculated for upward heat flow (from warm central regions toward the surface of the waste) and for downward heat flow (from warm central regions toward the bottom liner or base of the waste pile). Thermal losses due to convection (i.e., fluid flow) were omitted in the analysis based on (i) lack of detailed leachate generation/flow data for MSW at the sites included in this study, (ii) limited information on heat transfer through convective air flow in mining waste piles at the sites included in this study, and (iii) findings provided by Yesiller et al. (2005) indicating that convective losses due to leachate flow accounted for only 5% of total thermal losses for MSW. Thermal losses accumulate with time, and were calculated and reported herein for a period of 1 year (Tables 8 and 9). Conductive thermal losses in MSW ranged from 13 to 276 MJ/m^3 yr, whereas the range of conductive thermal losses was 19–1111 MJ/m^3 yr in mining wastes. The conductive thermal losses for the MSW incinerator ash landfill in Germany were calculated to be 973 MJ/m^3 yr.

The analysis and data provided herein can be used to determine total heat generation for periods other than 1 year. The total heat energy generated, E_{total}, can be calculated using Eq. (3). L_t may vary with time due to changes in thermal regime of the waste mass, particularly for cases with extended analysis periods.

$$E_{total} = E_{heating} + nL_t \quad (3)$$

where $E_{heating}$ is energy production for heating waste (MJ/m^3), L_t is thermal losses to the surrounding environment (MJ/m^3 yr), and n is number of years. Overall, the thermal losses constituted a significant component of total heat energy generated.

The calculation of total heat energy as presented above provides a mechanistic-empirical methodology. Young (1992) presented a theoretical approach whereby the total energy generated in MSW

Table 8
Heat generation: MSW.

Source	Site/location	Peak average temperature differential (°C/day/day)	Peak average heat generation, $E_{heating}$ (MJ/m^3)	Average excess heat energy above mesophilic conditions (MJ/m^3)	Conductive losses (MJ/m^3 yr)	Waste age (years)
Rees (1980a)	Aveley Landfill (near Essex, UK)	22.6	29.4	1.2 to −5.3	276.4	3 to 5
Houi et al. (1997)	Montech Landfill (near Toulouse, France)	30.0	18.0	7.5 to 4.5	12.9	0 to 2
Lefebvre et al. (2000)	Montech Landfill (near Toulouse, France)	30.6	18.3	7.9 to 4.9	19.1	0 to 1
Koerner (2001)	(near Philadelphia, Pennsylvania, USA)	3.4	6.0	−30.3 to −39.0	23.3	0 to 7
Yoshida and Rowe (2003)	Tokyo Port Landfill (Tokyo, Japan)	17.8	39.2	6.0 to −5.0	30.5	7 to 17
Hanson et al. (2008)	Sauk Trail Hills Landfill (Canton, Michigan, USA)	41.6	83.1	40.0 to 29.9	147.1	4 to 11
Hanson et al. (2008)	Los Corralitos Regional Landfill (Las Cruces, New Mexico, USA)	6.1	7.3	−9.6 to −15.6	35.6	0 to 13
Hanson et al. (2008)	Anchorage Regional Landfill (Anchorage, Alaska, USA)	32.2	32.1	2.9 to −2.1	18.7	8 to 16
Hanson et al. (2008)	Vancouver Landfill (Delta, British Columbia, Canada)	11.1	24.4	−22.0 to −24.3	127.3	3 to 13
Bouazza et al. (2011)	(Southeast of Melbourne, Australia)	35.5	46.2	24.5 to 18.0	85.1	0 to 1.5
Bonany et al. (2013)	(Ste. Sophie, Quebec, Canada)	−9.3	−8.6	−32.7 to −37.3	[-]	0 to 2
NP	Santa Maria Regional Landfill (Santa Maria, California, USA)	20.3	20.3	2.5 to −2.6	120.9	3 to 5
NP	Cold Canyon Landfill (San Luis Obispo, California, USA)	32.1	32.1	15.1 to 10.1	16.8	0 to 17

[-] – Frozen waste.
NP – Not previously published.

Table 9
Heat generation: mining waste.

Source	Type of waste	Site/location	Peak average temperature differential (°C/day/day)	Peak average heat generation, $E_{heating}$ (MJ/m^3)	Conductive heat losses (MJ/m^3 yr)	Pyrite mass fraction (%)	Waste age (years)
Harries and Ritchie (1981)	Uranium Mining Waste	Rum Jungle (Batchelor, Northern Territory, Australia)	25.8	37.4	181.7	3	20
Lefebvre et al. (1997)	Gold Mining Waste	Doyon Mine (Rouyn-Noranda, Quebec, Canada)	38.4	72.6	251.4	1.5 to 7	0 to 2
Lefebvre et al. (2001)	Gold Mining Waste	Doyon Mine (Rouyn-Noranda, Quebec, Canada)	22.0	35.9	360.5	1.5 to 7	0 to 15
Lefebvre et al. (2001)	Uranium Mining Waste	Nordhalde Waste Pile (Ronnenberg Mining District, Thuringia, Germany)	0.4	0.6	18.9	1 to 2	0 to 25
Hollesen et al. (2009)	Coal Mining Waste	(Svalbard, Norway)	6.1	12.1	34.2	<1	20 to 22
Pham et al. (2013)	Diamond Mining Waste	Diavik Diamond Mine (Yellowknife, Northwest Territories, Canada)	2.3	4.7	180.3	>0.08	1 to 2
Blanco et al. (2013)	Mine Tailings	Monte Romero Mine (Huelva, Spain)	5.3	8.2	1111.2	12	28

due to methanogenesis was calculated as the summation of (i) energy produced that was used to heat the waste mass (equivalent to $E_{heating}$), (ii) energy used for evaporating water into vapor, and (iii) thermal losses to the surrounding environment (equivalent to L_t). Therefore, the E_{total} calculated using Eq. (3) represents a conservative estimate as the amount of energy produced due to methanogenesis is expected to be higher due to the additional energy associated with evaporating water.

For MSW, additional analysis was conducted to determine the amount of excess heat energy above mesophilic conditions (Table 8) for optimizing alternative energy potential of a given MSW facility. In this analysis, excess energy above 35–40 °C, which was reported to be the optimum temperature range for maximum gas production in MSW, was calculated. This excess heat energy provides a second alternative energy source from a MSW landfill facility while maintaining optimum landfill gas generation conditions. The excess heat energy at the sites analyzed ranged from −39.0 to 40.0 MJ/m^3 yr. While the majority of the excess heat energy values were positive indicating waste temperatures above mesophilic conditions, negative values also were obtained indicating waste temperatures below mesophilic conditions. For cases with negative excess heat energy, heat would need to be provided to the waste mass to raise the waste temperatures to mesophilic conditions for optimum gas generation. Additional analysis could be conducted by applying this general methodology for other types of wastes or for other temperature thresholds for comprehensive heat management of waste containment systems.

6. Summary and conclusions

A comprehensive review of heat generation in various types of wastes and of the thermal regime of waste containment facilities was provided. Municipal solid waste, MSW incineration ash, and mining wastes were included in the analysis. Disposal sites located in multiple climatic regions and waste ages varying from less than 1 year to over several decades were included in the analysis. Spatial and temporal variations of waste temperatures, thermal gradients, thermal properties of wastes, average temperature differentials, and heat generation values were provided.

Heat generation was influenced by climatic conditions, mean annual earth temperatures, waste temperatures at the time of placement, cover conditions, and inherent heat generation potential of the specific wastes. Additional factors such as significant variations in waste composition and leachate and gas management practices also could potentially influence waste heat generation. Time to onset of heat generation varied between months and years, whereas timelines for overall duration of heat generation varied between years and decades. For MSW, measured waste temperatures were as high as 60–90 °C and as low as −6 °C. MSW incinerator ash temperatures varied between 5 and 87 °C. Mining waste temperatures were in the range of −25 to 65 °C. In temperate climates, combined high waste temperatures at time of placement (generally corresponding to seasonal high air temperatures) and high precipitation resulted in the highest waste temperatures, whereas in cold regions, high waste temperatures at time of placement and optimum precipitation resulted in high waste temperatures. An inverse relationship was observed between rate of temperature change and time for MSW where the rate of temperature change decreased with time. The time rates of temperature change were on the order of 40 °C/yr and −1 to 3 °C/yr for fresh (i.e., young) and old wastes, respectively. In the wastes analyzed, upward heat flow toward the surface was more prominent than downward heat flow toward the subsurface. Shallow zone thermal gradients generally ranged from 1 to 16 °C/m (MSW), was 23 °C/m (incinerator ash), and ranged from 1 to 4 °C/m (mining waste rock). Deep zone thermal gradients ranged from −13 to 0 °C/m (MSW), was −8.8 °C/m (incinerator ash), and ranged from −3.3 to 0 °C/m (mining waste). Based on thermal properties, MSW had insulative qualities with low thermal conductivity, while mining wastes typically were relatively conductive (high thermal conductivity) with ash having intermediate qualities.

The $\Delta T_{avg\text{-}peak}$ ranged from −9.3 to 41.6 °C-day/day for MSW, was 49.7 °C-day/day for MSW incinerator ash, and ranged from 0.4 to 38.4 °C-day/day for mining waste. The one-year peak average temperature differential ($\Delta T_{avg\text{-}peak\text{-}one\,year}$) was determined for the same depth as $\Delta T_{avg\text{-}peak}$ and ranged from 9.1 to 49.2 °C-day/day for MSW, was 75.9 °C-day/day for MSW incinerator ash, and ranged from 1.7 to 39.0 °C-day/day for mining waste. The baseline heat generation values ranged from −8.6 to 83.1 MJ/m^3 and from 0.6 to 72.6 MJ/m^3 for MSW and mining waste, respectively and the baseline heat generation was 72.6 MJ/m^3 for ash waste. Conductive thermal losses were determined to range from 13 to 1111 MJ/m^3 yr. Available excess heat energy above mesophilic conditions for most cases varied between 1 and 40 MJ/m^3 for MSW. The excess heat energy provides a second alternative energy source from a MSW landfill facility while maintaining optimum landfill gas generation conditions. The data and analysis provided in this review paper can be used in the investigation of heat generation and thermal regime and development of heat management strategies for a wide range of wastes and waste containment facilities located in different climatic regions.

Acknowledgements

The funds for the data obtained by the authors were provided by the National Science Foundation (GOALI Grant: CMS-9813248, SGER Grant: CMS-0301032, and a 2004 AAAS/NSF WISC Grant), the City of Santa Maria, California, and Cold Canyon Landfill, California. Cooperation of all partnering landfills is appreciated. Funding also was provided by the Global Waste Research Institute at California Polytechnic State University. Ms. Yee was supported by funds provided by a National Science Foundation REU Site Grant: EEC-1263337.

References

Abuel-Naga, H.M., Bouazza, A., 2013. Thermomechanical behavior of saturated geosynthetic clay liners. J. Geotech. Geoenviron. Eng., ASCE 139 (4), 539–547.

Barry, R.C., 2008. Gas-phase mass transfer processes in landfill microbiology. J. Environ. Eng., ASCE 134 (3), 191–199.

Bennett, J.W., Garvie, A.M., Pantelis, G., Ritchie, A.I.M., Bell, A.V., Noel, M., 1995. Comparison between measured and predicted transport processes controlling oxidation in the waste rock piles at the Heath Steele Mine site. In: Proceedings, Sudbury 95 Conference on Mining and the Environment, Sudbury, Ontario, Canada, pp. 1017-1026.

Blackford, M.G., Harries, J.R., 1985. A Heat Source Probe for Measuring Thermal Conductivity in Waste Rock Dumps. AAEC Report No. E609. Australian Atomic Energy Commission, Research Establishment, Lucas Heights Research Laboratories, NSW, Australia.

Blanco, A., Lloret, A., Carerra, A., Olivella, S., 2013. Thermo-hydraulic behaviour of the vadose zone in sulphide tailings at Iberian Pyrite Belt: Waste characterization, monitoring and modelling. Eng. Geol., Elsevier 165, 154–170.

Bonany, J., Van Geel, P.J., Gunay, H.B., Isgor, O.B., 2013. Heat budget for a waste lift placed under freezing conditions in a landfill operated in a northern climate. Waste Manage., Elsevier 33, 1215–1228.

Bouazza, A., Nahlawi, H., Aylward, M., 2011. In situ temperature monitoring in an organic-waste landfill cell. J. Geotech. Geoenviron. Eng., ASCE 137 (12), 1286–1289.

Cecchi, F., Pavan, P., Musacco, A., Mata-Alvarez, J., Vallini, G., 1993. Digesting the organic fraction of municipal solid waste: Moving from mesophilic (37 °C) to thermophilic (55 °C) conditions. Waste Manage. Res., ISWA 11, 403–414.

Chakma, S., Mathur, S., 2013. Postclosure long-term settlement for MSW landfills. J. Hazard. Toxic Radioactive Waste, ASCE 17 (2), 81–88.

Da Silva, J.C., Vargas, E.A., Sracek, O., 2009. Modeling multi-phase reactive transport in a waste rock pile with convective oxygen supply. Vadose Zone J. 8 (4), 1038–1050.

DeWalle, F.B., Chian, E.S.K., Hammerberg, E., 1978. Gas production from solid waste in landfills. J. Environ. Eng. Div., ASCE 104 (EE3), 415–432.

El-Fadel, M., Findikakis, A.N., Leckie, J.O., 1996. Numerical modelling of generation and transport of gas and heat in sanitary landfills: I. Model formulation. Waste Manage. Res., ISWA 14, 483–504.

Hanson, J.L., Edil, T.B., Yesiller, N., 2000. Thermal properties of high water content materials. In: Edil, T.B., Fox, P.J. (Eds.), Geotechnics of High Water Content Materials, ASTM STP 1374. ASTM, pp. 137–151.

Hanson, J.L., Yesiller, N., Howard, K.A., Liu, W.-L., Cooper, S.P., 2006. Effects of placement conditions on decomposition of municipal solid wastes in cold regions. In: Proceedings, 13th Annual Cold Regions Engineering Conference, ASCE, pp. 1–11.

Hanson, J.L., Liu, W.-L., Yesiller, N., 2008, Analytical and numerical methodology for modeling temperatures in landfills. In: Khire, M.V., et al. (Eds.), Geotechnics of Waste Management and Remediation, ASCE GSP 177. ASCE, pp. 24–31.

Hanson, J.L., Yesiller, N., Oettle, N.K., 2010. Spatial and temporal temperature distributions in municipal solid waste landfills. J. Environ. Eng., ASCE 136 (8), 804–814.

Harries, J.R., Ritchie, A.I.M., 1981. The use of temperature profiles to estimate the pyritic oxidation rate in a waste rock dump from an opencut mine. Water Air Soil Pollut. 15, 405–423.

Hartz, K.E., Klink, R.E., Ham, R.K., 1982. Temperature effects: Methane generation from landfill samples. J. Environ. Eng., ASCE 108 (EE4), 629–638.

Hollesen, J., Elberling, B., Hansen, B.U., 2009. Modelling subsurface temperatures in a heat producing coal waste rock pile, Svalbard (78°N). Cold Regions Sci. Technol., Elsevier 58, 68–76.

Hollesen, J., Elberling, B., Jansson, P.E., 2011. Modelling temperature-dependent heat production over decades in High Arctic coal waste rock piles. Cold Regions Sci. Technol., Elsevier 65, 258–268.

Houi, D., Paul, E., Couturier, C., 1997. Heat and mass transfer in landfills and biogas recovery. In: Christensen, T.H., et al. (Eds.), Proceedings, Sardinia 1997, Sixth International Waste Management and Landfill Symposium, vol. I. CISA, Italy, pp. 101–108.

Hudson, A.P., 2007. Evaluation of the Vertical and Horizontal Hydraulic Conductivities of Household Wastes. Ph.D. Thesis, University of Southampton.

Ishimori, H., Katsumi, T., 2012. Temperature effects on the swelling capacity and barrier performance of geosynthetic clay liners permeated with sodium chloride solutions. Geotextiles Geomembranes, Elsevier 33, 25–33.

Jafari, N.H., Stark, T.D., Rowe, R.K., 2014. Service life of HDPE geomembranes subjected to elevated temperatures. J. Hazard. Toxic Radioactive Waste, ASCE 18 (1), 16–26.

Kjeldsen, P., Christensen, T.H., 2001. A simple model for the distribution and fate of organic chemicals in a landfill: MOCLA. Waste Manage. Res., ISWA 19, 201–216.

Klein, R., Baumann, T., Kahapka, E., Niessner, R., 2001. Temperature development in a modern municipal solid waste incineration (MSWI) bottom ash landfill with regard to sustainable waste management. J. Hazard. Mater., Elsevier B83, 265–280.

Klein, R., Nestle, N., Niessner, R., Baumann, T., 2003. Numerical modelling of the generation and transport of heat in a bottom ash monofill. J. Hazard. Mater., Elsevier B100, 147–162.

Koerner, G., 2001. In situ temperature monitoring of geosynthetics used in a landfill. Geotech. Fabrics Rep., IFAI 19 (4), 12–13.

Koerner, R.M., Koerner, G.R., 2014. Monitoring in-situ conditions at landfills for the purpose of evaluating long term geomembrane performance. In: Proceedings, 10th International Conference on Geosynthetics, IGS, pp. 1–5.

Lahmira, B., Barbour, L., Huang, M., 2014. Numerical modeling of gas flow in the Suncor coke stockpile covers. Vadose Zone J. 13 (1). http://dx.doi.org/10.2136/vzj2013.07.0119.

Lamothe, D., Edgers, L., 1994. The effects of environmental parameters on the laboratory compression of refuse. In: Proceedings, Seventeenth International Madison Waste Conference. Department of Engineering Professional Development, University of Wisconsin, Madison, WI, pp. 592–604.

Lefebvre, R., Gelinas, P., Isabel, D., 1997. Heat Transfer during Acid Mine Drainage Production in a Waste Rock Dump, La Mine Doyon (Quebec), MEND Research Program Report 1.14.2c, CANMET, Ottawa, Canada, March 1994, Revised August 1997.

Lefebvre, R., Hockley, D., Smolensky, J., Gelinas, P., 2001. Multiphase transfer processes in waste rock piles producing acid mine drainage 1: Conceptual model and system characterization. J. Contam. Hydrol., Elsevier 52, 137–164.

Lefebvre, X., Lanini, S., Houi, D., 2000. The role of aerobic activity on refuse temperature rise, I. Landfill experimental study. Waste Manage. Res., ISWA 18, 444–452.

Lowry, M.I., Bartelt-Hunt, S.L., Beaulieu, S.M., Barlaz, M.A., 2008. Development of a coupled reactor model for prediction of organic contaminant fate in landfills. Environ. Sci. Technol., ACS 42 (19), 7444–7451.

Mata-Alvarez, J., Martinez-Viturtia, A., 1986. Laboratory simulation of municipal solid waste fermentation with leachate recycle. J. Chem. Technol. Biotechnol. 36, 547–556.

Nunoo, S., 2009. Geotechnical Evaluation of Questa Mine Material Taos County, New Mexico. M.S. Thesis, New Mexico Institute of Mining and Technology.

ORNL, 1981. Regional Analysis of Ground and Above-Ground Climate. Oak Ridge National Laboratory Report No. ORNL/Sub-81/40451/1, U.S. Department of Energy, Office of Buildings Energy R&D.

Peel, M.C., Finlayson, B.L., McMahon, T.A., 2007. Updated world map of the Koppen–Geiger Climate Classification. Hydrol. Earth Syst. Sci. 11, 1633–1644.

Pham, N., Sego, D., Blowes, D., Amos, R., Smith, L., 2011. Diavik Waste Rock Project: Thermal transport in a covered waste rock test pile. In: Proceedings, Tailings and Mine Waste 2011, Vancouver, Canada, pp. 1–14.

Pham, N.H., Sego, D.C., Arenson, L.U., Blowes, D.W., Amos, R.T., Smith, L., 2013. The Diavik Waste Rock Project: Measurement of the thermal regime of a waste-rock test pile in a permafrost environment. Appl. Geochem., Elsevier 36, 234–245.

Rees, J.F., 1980a. The fate of carbon compounds in the landfill disposal of organic matter. J. Chem. Technol. Biotechnol., Society of Chemical Industry 30, 161–175.

Rees, J.F., 1980b. Optimisation of methane production and refuse decomposition in landfills by temperature control. J. Chem. Technol. Biotechnol., Society of Chemical Industry 30, 458–465.

Sawamura, H., Yamada, M., Endo, K., Soda, S., Ishigaki, T., Ike, M., 2010. Characterization of microorganisms at different landfill depths using carbon-utilization patterns and 16S rRNA gene based T-RFLP. J. Biosci. Bioeng., Elsevier 109 (2), 130–137.

Smith, M., Glasser, D., 2005. Spontaneous combustion of carbonaceous stockpiles. Part I: The relative importance of various intrinsic coal properties and properties of the reaction system. Fuel, Elsevier 84, 1151–1160.

Smith, L.J.D., Blowes, D.W., Jambor, J.L., Smith, L., Sego, D.C., Neuner, M., 2013. The Diavik Waste Rock Project: Particle size distribution and sulfur characteristics of low-sulfide waste rock. Appl. Geochem. 36, 200–209.

Southen, J.M., Rowe, R.K., 2005. Modeling of thermally induced desiccation of geosynthetic clay liners. Geotextiles Geomembranes, Elsevier 23 (5), 425–442.

Spokas, K., Bogner, J., Chanton, J., 2011. A process-based inventory model for landfill CH_4 emissions inclusive of seasonal soil microclimate and CH_4 oxidation. J. Geophys. Res., AGU 116, G04017.

Sracek, O., Choquette, M., Gelinas, P., Lefebvre, R., Nicholson, R.V., 2004. Geochemical characterization of acid mine drainage from a waste rock pile, Mine Doyon, Quebec, Canada. J. Contam. Hydrol., Elsevier 69, 45–71.

Stark, T.D., Martin, J.W., Gerbasi, G.T., Thalhamer, T., Gortner, R.E., 2012. Aluminum waste reaction indicators in a municipal solid waste landfill. J. Geotech. Geoenviron. Eng., ASCE 138 (3), 252–261.

Tan, Y., Ritchie, A.I.M., 1997. In situ determination of thermal conductivity of waste rock dump material. Water Air Soil Pollut. 98, 345–359.

Tchobanoglous, G., Theisen, H., Vigil, S.A., 1993. Integrated Solid Waste Management: Engineering Principles and Management Issues. McGraw Hill Inc, New York, NY.

Wels, C., Lefebvre, R., Robertson, A.M., 2003. An overview of prediction and control of air flow in acid-generating waste rock dumps. In: Proceedings, Sixth International Conference on Acid Rock Drainage (6th ICARD), Cairns, Queensland, Australia, pp. 639–650.

Yesiller, N., Hanson, J.L., Liu, W.-L., 2005. Heat generation in municipal solid waste landfills. J. Geotech. Geoenviron. Eng., ASCE 131 (11), 1330–1344.

Yesiller, N., Hanson, J.L., Yoshida, H., 2011. Landfill temperatures under variable decomposition conditions. In: Han, J., Alzamora, D.E. (Eds.), Advances in Geotechnical Engineering, ASCE GSP 211. ASCE, pp. 1055–1065.

Yoshida, H., Rowe, R.K., 2003. Consideration of landfill liner temperature. In: Christensen, T.H. et al. (Eds.), Proceedings, Sardinia 2003, Ninth International Waste Management and Landfill Symposium, CISA, Italy, pp. 1–8.

Yoshida, H., Tanaka, N., Hozumi, H., 1997. Theoretical study on heat transport phenomena in a sanitary landfill. In: Christensen, T.H. et al. (Eds.), Proceedings, Sardinia 1997, Sixth International Waste Management and Landfill Symposium. CISA, Italy, pp. 109–120.

Young, A., 1992. Application of Computer Modelling to Landfill Processes. DoE Report No. CWM 039A/92, Department of Environment (UK).

Zambra, C.E., Moraga, N.O., 2013. Heat and mass transfer in landfills: Simulation of the pile-self heating and of the soil contamination. Int. J. Heat Mass Transfer, Elsevier 66, 324–333.

Zanetti, M.C., Manna, L., Genon, G., 1997. Biogas production evaluation by means of thermal balances. In: Christensen, T.H. et al. (Eds.), Proceedings, Sardinia 1997, Sixth International Waste Management and Landfill Symposium, vol. II, CISA, Italy, pp. 523–531.